第34卷 第6期 焊 接 学 报 Vol. 34 No. 6
2013年6月 TRANSACTIONS OF THE CHINA WELDING INSTITUTION June 2013

高温合金 GH4169 真空扩散连接工艺

李卓然[1]， 冯广杰[1]， 徐 慨[1]， 张相龙[1]， 刘 兵[2]， 于 康[3]
(1. 哈尔滨工业大学 先进焊接与连接国家重点实验室，哈尔滨 150001;
2. 上海飞机制造有限公司，上海 200436; 3. 上海空间推进研究所，上海 200233)

摘 要：采用真空直接扩散以及加镍中间层对高温合金 GH4169 进行了连接，阐述了扩散连接工艺参数对接头界面和接头力学性能的影响，以孔隙的多少作为评价指标来说明工艺参数对接头的影响. GH4169 的直接扩散连接，升高加热温度、延长保温时间和增大连接压力均会不同程度的使界面的孔隙数目减少、尺寸变小. 连接温度 1 100 ℃，保温时间 90 min，连接压力 40 MPa 时，扩散孔隙基本消失，接头平均抗拉强度达到 658 MPa. 采用镍中间层对 GH4169 进行扩散连接，接头塑性得到改善，接头抗拉强度得到明显提高；连接温度 990 ℃，保温时间 75 min，连接压力 15 MPa 时，接头抗拉强度达到 840 MPa.

关键词：镍基合金； 真空扩散连接； 镍中间层； 抗拉强度
中图分类号：TG453 **文献标识码**：A **文章编号**：0253－360X(2013)06－0021－04

李卓然

0 序 言

GH4169 是复杂的多元第二相强化类镍基高温合金，作为以 γ'' 相强化为主，δ 相强化为辅的时效强化类高温合金，具有良好的室温和高温强度、刚度、塑性以及良好的疲劳性能等，使得 GH4169 在工业生产中的到了广泛的应用[1-3]. 据统计 GH4169 合金的产量占锻造高温合金的 50%，广泛用于制造导向叶片、涡轮盘、燃烧室等多种结构性和功能性的重要零件. 因此 GH4169 镍基高温合金在整个高温合金领域内占有特殊的重要地位，是国计民生中应用最广泛、地位最重要的材料之一[4-6].

文中采用真空扩散连接以及加中间层镍箔实现了 GH4169 自身的连接，系统分析了扩散连接工艺参数对界面扩散孔隙及抗拉性能的影响，从而确定的两种连接条件下的扩散连接工艺参数.

1 试验方法

试验所采用的材料为锻造态 GH4169 合金棒材，锻态 GH4169 合金的基体为 γ 相，是面心立方结构的镍基奥氏体相，基体中存在大量形变孪晶，以及在冶炼过程中残留的灰白色块状铌和钛的氮(碳)化物夹杂颗粒、块状的碳化铌(NbC)颗粒和氮化钛(TiN)颗粒，尺寸为 520 μm. 采用的中间层镍箔厚度为 10 μm.

焊前需去除合金表面的氧化膜. 试验采用化学酸洗的方法去膜，腐蚀液配比按体积比 HCl: HNO_3: H_2O: H_2O_2 = 2: 2: 2: 1 的比例配置，现配现用. 化学酸洗后的母材在丙酮中超声清洗 10 min，装配之前取出吹干.

试验所采用的焊接工艺曲线如图 1 所示. 采用电子扫描显微镜(SEM，S-4700)对接头界面形貌和组织进行观察以及能谱分析. 采用电子万能试验机(Instron Model 1186)进行强度拉伸试验.

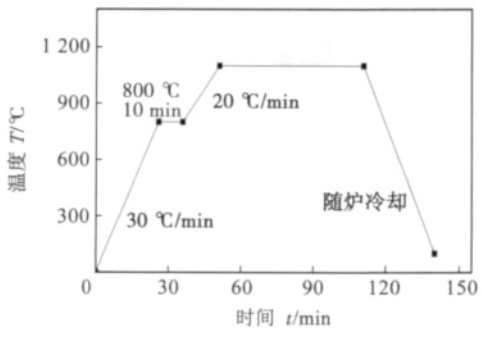

图 1 扩散连接试验工艺曲线

Fig. 1 Cycle curve of diffusion bonding

收稿日期：2012－05－03
基金项目：国家自然科学基金资助项目(51075101)

2 试验结果与讨论

2.1 GH4169 合金真空直接扩散连接

图 2 为连接温度 1 100 ℃,保温时间 90 min,连接压力 30 MPa 时,GH4169 合金真空直接扩散连接接头典型的界面组织形貌. 从图 2 中可以看出,接头界面处没有反应层的生成,仅有扩散孔隙的存在,扩散连接的过程也就是孔隙的闭合过程.

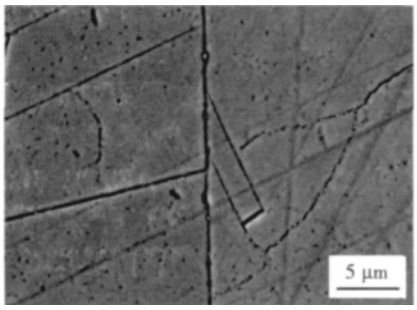

图 2 接头微观组织形貌

Fig. 2 Microstructure of joint

图 3 为连接压力 30 MPa,保温时间 90 min 条件下,连接温度分别为 1 020 ℃ 和 1 100 ℃ 接头微观组织形貌. 从图 3 中可以看出,当连接温度为 1 020 ℃ 时,接头界面处扩散孔隙数量较多且尺寸较大,连接温度较低使金属原子间的扩散不充分. 对其进行室温拉伸强度试验结果如图 4 所示,接头的平均抗拉强度为 386 MPa. 随着温度的升高,界面处元素扩散逐渐充分,接头界面处扩散空隙数量逐渐减少且尺寸逐渐减小; 当连接温度为 1 100 ℃ 时,接头界面处扩散空隙数量明显减少且尺寸已接近晶界尺寸,表明此条件下金属原子间的扩散较充分,被连接材料在界面处易达到原子间紧密接触. 对其进行室温拉伸强度试验,接头的平均抗拉强度为 627 MPa,接头强度有了明显改善.

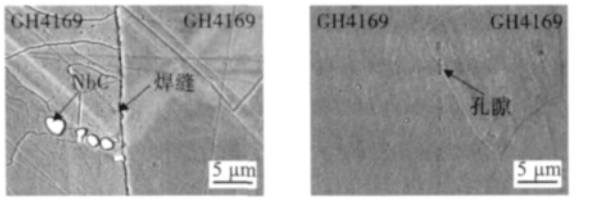

(a) 接头界面形貌 (T=1 020 ℃) (b) 接头界面形貌 (T=1 100 ℃)

图 3 连接温度对界面扩散孔隙的影响

Fig. 3 Effects of diffusion bonding temperature on diffusion holes

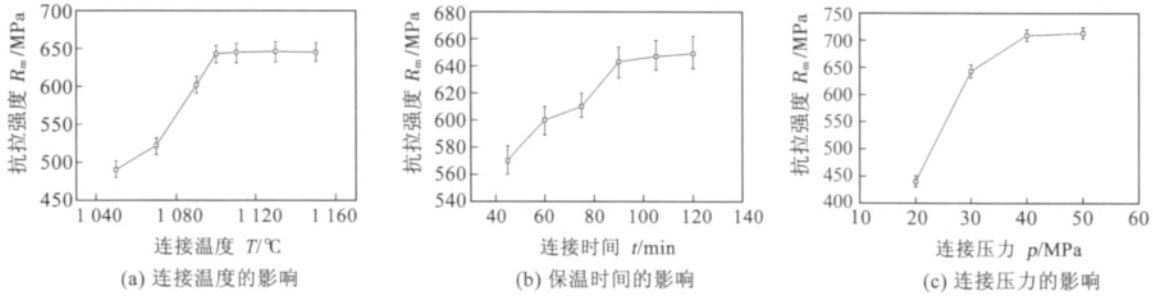

(a) 连接温度的影响 (b) 保温时间的影响 (c) 连接压力的影响

图 4 扩散连接工艺参数对接头性能的影响

Fig. 4 Effects of diffusion bonding parameters on mechanical properties of joints

在一定的连接温度和连接压力条件下,连接时间较短时,原子之间的扩散不充分,不能形成理想的接头,接头强度较低; 随着时间的延长,原子扩散逐渐充分,接头强度增加,但连接时间过长,容易造成接头区域晶粒长大.

由于 GH4169 高温合金在高温时依然有较高的力学性能,在连接压力较低时,接头界面很难达到原子间的紧密接触,使金属原子间的扩散不充分,孔洞闭合不充分. 对其进行室温拉伸强度试验,接头的平均抗拉强度为 485 MPa. 随着连接压力的升高,界面处逐渐发生较大的塑性变形,达到紧密的接触,接头界面处扩散孔隙的闭合速度增快使孔隙数量减少,尺寸减小; 当连接压力达到 40 MPa 时,接头界面处扩散孔隙基本消失且尺寸已接近晶界尺寸,表明此条件下,被连接材料在界面处易达到原子间紧密接触,金属原子间的扩散较充分. 对其进行室温拉伸强度试验,接头的平均抗拉强度为 658 MPa,接头强度有了明显改善.

图 5 为连接温度 1 100 ℃, 保温时间 90 min,连接压力 30 MPa 时,GH4169 合金真空直接扩散连接

接头的断口形貌. 从图 5 中可以看出,直接扩散连接断口为典型的解理面,是典型的脆性断裂.

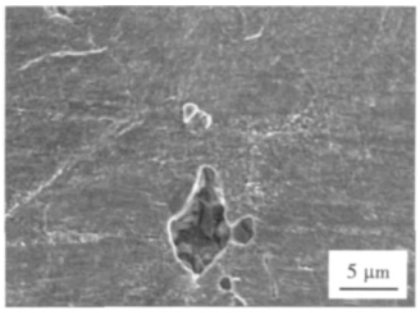

图 5　接头断口形貌

Fig. 5　Fracture surface of joint

2.2　加镍中间层的 GH4169 真空扩散连接

通过以上试验及其分析可知,直接扩散连接需要较高的温度、较大的压力,才能实现可靠的连接. 因此采用加镍箔中间层的方法对 GH4169 合金进行扩散连接. 由于镍箔具有较好的韧性和延展性,在高温下屈服强度较低,作为软质中间层进行扩散连接,可以增强被连接面之间的紧密接触程度及相互作用,这就为接头原子扩散提供了便利条件.

图 6 为连接温度分别为 900,990 ℃,保温时间 90 min,连接压力 20 MPa 时得到的扩散连接接头的背散射图片. 从图 6 中可以看出,接头界面处仅存在扩散孔隙. 当温度较低时,接头界面处的扩散孔隙数量较多,尺寸较大且连续分布,随着温度的逐渐提高,接头界面处的扩散孔隙越来越少,焊合的界面越来越多; 当温度达到 990 ℃时,接头界面处的扩散孔隙完全消失,镍箔与 GH4169 合金的界面模糊,整个接头达到良好连接.

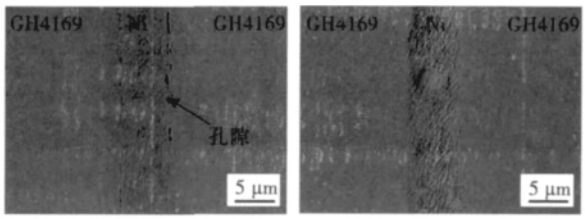

(a) 接头界面形貌 (T=900 ℃)　(b) 接头界面形貌 (T=990 ℃)

图 6　连接温度对接头界面扩散孔隙的影响

Fig. 6　Effects of diffusion bonding temperature on diffusion holes

图 7 为扩散连接温度和保温时间对加镍箔中间层 GH4169 合金真空扩散连接接头抗拉强度的影响. 当扩散连接温度为 90 min,连接压力为 20 MPa 时,随着扩散连接温度的升高,接头的抗拉强度迅速升高; 当扩散温度达到 990 ℃时,接头抗拉强度达到 885 MPa; 随后扩散连接温度继续升高,接头的抗拉强度基本不变. 在接头拉伸过程中,镍箔中间层具有较好的韧性,屈服应力升高,变形抗力增大,故接头强度升高.

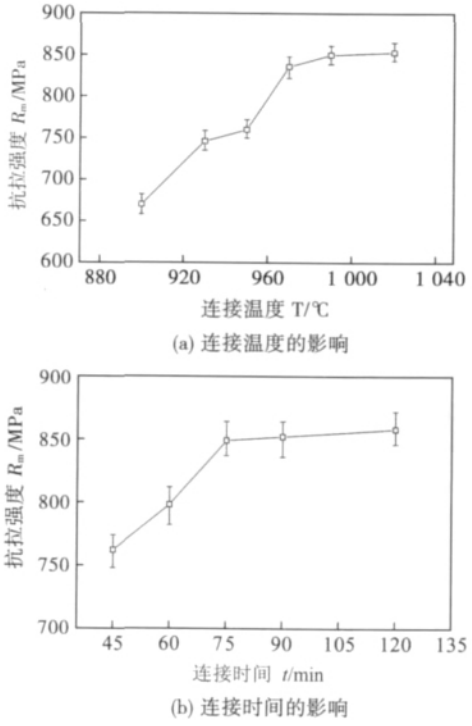

图 7　扩散连接工艺参数对接头性能的影响

Fig. 7　Effects of diffusion bonding parameters on mechanical properties of joints

由于界面处只有扩散孔隙的存在,因此接头抗拉强度随扩散温度产生的这种变化是由界面扩散是否充分和扩散孔隙数量和大小决定的. 当扩散连接温度较低时,GH4169 合金与镍箔中间层之间的原子扩散不充分,孔隙数量较多、尺寸较大且连续分布. 当扩散温度为 990 ℃左右时,界面原子扩散充分,界面孔隙消失,接头获得良好的力学性能.

图 8 为扩散连接温度 990 ℃,保温时间 75 min,连接压力 15 MPa 时,加 10 μm 纯镍箔中间层间接扩散连接接头典型断口形貌. 宏观断口分为 A 和 B 两个明显特征区域. 为了具体分析接头的断裂位置,对区域进行微观放大,并进行了能谱分析. A 区断裂面有一定韧窝,经能谱面分析其化学成分为 91.30Ni-4.84Cr-1.49Fe-1.49Ti-0.7Nb,由此可知,A 区断裂面上主要为纯镍层. 由 B 区的能谱结果 (69.53Ni-24.03Cr-1.33Fe-2.88Nb-1.24Ti),结合

Ni-Cr 二元相图可知，其断裂面上为(Ni，Cr)固溶体，合金中的 Cr 原子扩散到了 10 μm 厚镍箔中.

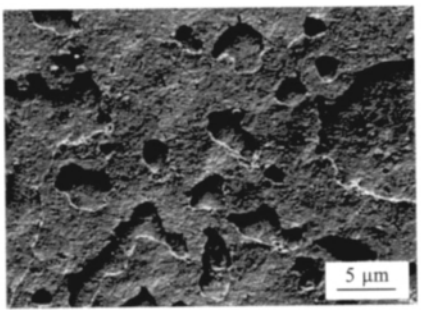

图 8 扩散连接接头断口形貌

Fig. 8 Fracture surface of joint

为进一步确定接头界面断裂位置，对加镍中间层的 GH4169 合金间接扩散连接断口进行 X 射线衍射试验，结果如图 9 所示. X 射线结果表明，接头断口主要为镍层和 Cr_2Ni_3，接头断裂位置在镍箔中间层处.

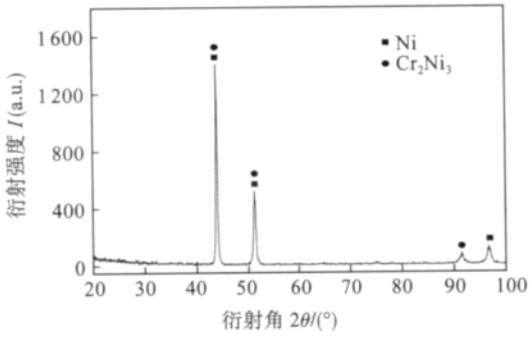

图 9 接头断口 X 射线衍射结果

Fig. 9 XRD result of fracture surface

3 结 论

(1) GH4169 真空直接扩散连接时，在连接温度为 950 ~ 1 150 ℃ 范围内，随着温度的升高，保温时间的延长和连接压力的增大，界面扩散孔隙数量逐渐降低且尺寸变小.

(2) GH4169 真空直接扩散连接时，当连接温度达到 1 100 ℃，保温时间为 90 min，连接压力为 40 MPa 时，扩散孔隙基本消失，接头强度达到 658 MPa，接头断裂形式为脆性断裂.

(3) GH4169 加镍中间层真空扩散连接时，当连接温度达到 990 ℃，保温时间为 75 min，连接压力为 15 MPa 时，接头抗拉强度达到 840 MPa，高于直接扩散连接强度. 接头断裂部位在镍中间层，且接头塑性比直接扩散连接接头的塑性明显提高.

参考文献:

[1] 李卓然，于 康，刘 兵，等. GH4169 合金真空扩散连接接头的组织和性能[J]. 焊接学报，2010，31(11)：13 - 16.
Li Zhuoran，Yu Kang，Liu Bing，*et al*. Microstructure and properties of GH4169 vacuum diffusion bonded joint [J]. Transactions of the China Welding Institution，2010，31(11)：13 - 16.

[2] Slama C，Abdellaoui M. Structural characyerization of the aged Inconel 718 [J]. Alloys and Compounds，2000，306(1/2)：277 - 284.

[3] 王西昌，左从进，柴国明，等. 活性剂对 GH4169 薄板电子束焊接焊缝成形的影响[J]. 焊接学报，2009，30(2)：83 - 86.
Wang Xichang，Zuo Congjin，Chai Guoming，*et al*. Effect of activating fluxes on appearance of weld in thin plate electron beam welding of nickel-base super alloy GH4169 [J]. Transactions of the China Welding Institution，2009，30(2)：83 - 86.

[4] Takuya U，Naoki W，Yoshitaka H，*et al*. An atomistic study of grain boundary stability and crystal rearrangement using molecular dynamics techniques [J]. Mechanical Science，2008，50(5)：956 - 965.

[5] 李文亚，陈 亮，余 敏. GH4169 合金惯性摩擦焊接头温度场显式有限元数值模拟[J]. 焊接学报，2011，32(6)：61 - 64.
Li Wenya，Chen Liang，Yu Min. Numerical simulation on temperature field of inertia friction welded GH4169 joint by explicit finite element analysis [J]. Transactions of the China Welding Institution，2011，32(6)：61 - 64.

[6] Nalawade S A，Sundararaman M，Singh J B，*et al*. Precipatation of γ' phase in δ-precipitated alloy 718 during deformation at elevated temperature [J]. Materials Science and Engineering A，2010，527(12)：2906 - 2909.

作者简介：李卓然，男，1971 年出生，博士，副教授，博士研究生导师. 主要从事新材料及异种材料连接方面的研究. 发表论文 60 余篇. Email：lizr@hit.edu.cn

Key words: thermal spraying; residual stress; elasto-plastic; finite element modeling; shaft part

Decoupling control design and simulation of aluminum alloy pulsed MIG welding based on dynamic PLS framework

LÜ Yan[1], TIAN Xincheng[2], LIANG Jun[1] (1. State Key Laboratory of Industrial Control Technology, Zhejiang University, Hangzhou 310027, China; 2. Department of Control Science and Engineering, Shandong University, Jinan 250061, China). pp 17 – 20

Abstract: To overcome the multivariable strong-coupling and difficulties in modeling during pulsed MIG welding of aluminum alloy, this paper transferred the multivariable controller design in original space to multi-loop SISO controller design in latent space and designed PID controller for each control loop independently, based on the decoupling and modeling advantages of the dynamic PLS framework. The characteristics and structure of the controller design in this framework were introduced, and the simulation of aluminum alloy pulsed MIG welding was carried out. The results demonstrate that the controller design using the dynamic PLS framework can obtain satisfactory dynamic and steady characteristics, and can be applied to other welding processes. It provides basis for the application of dynamic modeling and control methods, based on data-driven, in complex welding processes.

Key words: aluminum alloy pulsed MIG welding; decoupling control; dynamic PLS; PID

Vacuum diffusion bonding of GH4169 superalloy

LI Zhuoran[1], FENG Guangjie[1], XU Kai[1], ZHANG Xianglong[1], LIU Bing[2], YU Kang[3] (1. State Key Laboratory of Advanced Welding and Joining, Harbin Institute of Technology, Harbin 150001, China; 2. Shanghai Aircraft Manufacturing Co., Ltd., Shanghai 200436, China; 3. Shanghai Institute of Space Propulsion, Shanghai 200233, China). pp 21 – 24

Abstract: GH4169 superalloy was bonded to itself by vacuum diffusion bonding with Ni interlayer. The effect of process parameters on the interface structure and mechanical properties of the joints was investigated. The bonding holes in the interface were used as the evaluation indicator. The experimental results without Ni interlayer show that, with the increase of heating temperature, diffusion time and diffusion pressure, the number and size of bonding holes in the interface decreased. When the bonding temperature was 1 100 ℃, the bonding time was 90 min and the pressure was 40 MPa, the diffusion holes almost disappeared, and the average tensile strength reached 658 MPa. With Ni interlayer, the briquettability of the joint was improved and the average tensile strength apparently increased. When the bonding temperature was 990 ℃, the bonding time was 75 min and the pressure was 15 MPa, the average tensile strength reached 840 MPa.

Key words: nickel-base alloy; vacuum diffusion bonding; Ni interlayer; tensile strength

Analysis on welding stability of twin deposition surfacing electrode

ZHAO Wei, ZOU Yong, ZOU Zengda, WANG Yufu (Key Laboratory of Liquid Structure and Heredity of Materials, Ministry of Education, Shandong University, Jinan 250061, China). pp 25 – 28

Abstract: The influences of the electrode parameters and welding parameters on the welding stability were investigated with ϕ 4.0 mm twin deposition surfacing electrode. The results show that the arc voltage was mainly determined by the distance between twin cores, but it was also affected by the droplet transfer and arc force. Welding with too small or too large distance between twin cores degraded the welding stability. When the distance between twin cores was 1.0 mm and the arc voltage was kept at around 33 V, the welding process was stable. When the weight coefficient of the coating was 45%-56%, the hardness of the cladding layer was over 6 200 MPa, with good protection and sufficient metallurgical reaction in the weld. The appropriate welding current should be controlled between 180-200 A, which was higher in magnitude but narrower in amplitude than that with traditional hard surfacing electrodes under the same specification. When the distance between the electrode and workpiece was 7 mm, excellent bonding between the weld and base metal was obtained with stable welding process.

Key words: twin deposition surfacing electrode; arc voltage; welding stability

Effect of rosin content on rosin-based fluxes for Zn20Sn solders

SHENG Yangyang, YAN Yanfu, ZHAO Kuaile, ZHAO Yongmeng (School of Materials Science and Engineering, Henan University of Science and Technology, Luoyang 471003, China). pp 29 – 32

Abstract: The poor wetting of zinc-based alloys has become the bottleneck restraining their extensive applications. In this paper, a new flux was produced by adding proper amounts of organic acid, solvent, corrosion inhibitor, and surface active agent to improve the wetting properties of Zn20Sn solder. The results showed that when the rosin content was within the range of 40%–60%, the physical stability, inadhesion and corrosion properties of the flux could meet the requirements of relevant national standards. With the increasing of the rosin content, the spreading area and spreading ratio of the Zn20Sn solder increased first and then decreased. When the rosin content was about 55%, the spreading area and spreading ratio of the Zn20Sn solder reached the maximum values as 70.3 mm^2 and 87%, respectively. And no apparent defects occurred in the resultant joint, indicating that the flux benefited to enhance the soldering effects of Zn20Sn solder.

Key words: flux; Zn20Sn solder; spreading area; spreading ratio

Analysis of interface fracture behavior of arc fusion-brazed joint between titanium and aluminum dissimilar alloys

LÜ Shixiong[1], CUI Qinglong[1], HUANG Yongxian[1], JING Xiaojun[2] (1. State Key Laboratory of Advanced Welding and Joining, Harbin Institute of Technology, Harbin 150001, China; 2. Chengdu SIWI High-Tech Industrialized Garden Co., Ltd., Chengdu 611731, China). pp 33 – 36

Abstract: Fusion-brazing of titanium alloy to aluminum alloy was achieved by TIG arc, and the interface microstructure and fracture characteristics of the joints made with different fillers were analyzed. The results indicate that the interface microstructure in the joints with pure Al filler consisted of $TiAl_3$ phase, and cracks initiated at the interface corner and propagated along the interface between $TiAl_3$ layer and welded seam. The facture style